Advances in Colloid and Interface Science 208 (2014) 214–224

Contents lists available at ScienceDirect

Advances in Colloid and Interface Science

journal homepage: www.elsevier.com/locate/cis

Wrapping of nanoparticles by membranes

Amir H. Bahrami [a], Michael Raatz [a], Jaime Agudo-Canalejo [a], Raphael Michel [b], Emily M. Curtis [c], Carol K. Hall [c], Michael Gradzielski [b], Reinhard Lipowsky [a], Thomas R. Weikl [a,*]

[a] Max Planck Institute of Colloids and Interfaces, Department of Theory and Bio-Systems, Science Park Golm, 14424 Potsdam, Germany
[b] Stranski-Laboratorium für Physikalische und Theoretische Chemie, Institut für Chemie, Technische Universität Berlin, 10623 Berlin, Germany
[c] Department of Chemical and Biomolecular Engineering, North Carolina State University, Engineering Building I, 911 Partners Way, Raleigh, NC 27695-7905, USA

ARTICLE INFO

Available online 12 March 2014

Keywords:
Nanoparticles
Membranes
Bending energy

ABSTRACT

How nanoparticles interact with biomembranes is central for understanding their bioactivity. Biomembranes wrap around nanoparticles if the adhesive interaction between the nanoparticles and membranes is sufficiently strong to compensate for the cost of membrane bending. In this article, we review recent results from theory and simulations that provide new insights on the interplay of bending and adhesion energies during the wrapping of nanoparticles by membranes. These results indicate that the interplay of bending and adhesion during wrapping is strongly affected by the interaction range of the particle–membrane adhesion potential, by the shape of the nanoparticles, and by shape changes of membrane vesicles during wrapping. The interaction range of the particle–membrane adhesion potential is crucial both for the wrapping process of single nanoparticles and the cooperative wrapping of nanoparticles by membrane tubules.

Contents

1. Introduction

Recent advances in nanotechnology have led to an increasing interest in how nanoparticles interact with living organisms [1]. On the one hand, biomedically designed nanoparticles are promising delivery vehicles or vectors in drug treatments [2–6]. On the other hand, nanoparticles are frequently incorporated into smart materials, in food packing, as antifouling agents or to keep surfaces sterile [7]. This wide application of industrial nanoparticles has also led to concerns about their safety [8,9,3] and has triggered intense activities to investigate and understand nanotoxicity [10–12].

Since nanoparticles have to cross biomembranes to enter the cells and organelles of living organisms, a current focus is on understanding the interactions of nanoparticles with membranes. Nanoparticles that are larger than the membrane thickness cross the membrane by

* Corresponding author.
E-mail address: thomas.weikl@mpikg.mpg.de (T.R. Weikl).

http://dx.doi.org/10.1016/j.cis.2014.02.012
0001-8686/

wrapping and subsequent fission of a membrane neck. The wrapping of nanoparticles by the membranes can either occur spontaneously from an interplay of adhesive and elastic energies, or can be assisted by the curvature-inducing proteins and protein machineries of cellular membranes [13–16].

The topic of this review is the spontaneous wrapping of nanoparticles by membranes. Spontaneous wrapping occurs if the adhesive interaction between the nanoparticles and the membrane is sufficiently strong to compensate for the cost of membrane bending. The spontaneous wrapping of nanoparticles has been observed in experiments with lipid vesicles [17–21], polymersomes [22,23], and cells [24,25], and has been investigated by theoretical calculations [26–39] and simulations [40–62]. In this review article, our focus is on recent results from theory and simulations that provide new insights on how the wrapping process is affected (i) by the interaction range of the particle–membrane adhesion potential, (ii) by the shape of the nanoparticles, and (iii) by shape changes of membrane vesicles during wrapping.

Previous theoretical investigations have been largely focused on particle–membrane adhesion potentials with an interaction range that is negligibly small compared to the particle dimensions. For nanoparticles, however, the interaction range of the adhesion potential can be several percent of the particle diameter. Such interaction ranges strongly affect the wrapping process of single particles (see Section 3) and can lead to the cooperative wrapping of particles in tubular membrane invaginations (see Section 6) [39]. These particle-filled membrane tubes have been recently observed by several groups in simulations [48,50,53].

Experiments indicate that the internalization of nanoparticles by cells is affected by the size and shape of the particles [63–69,46,70–73]. How the spontaneous wrapping of nanoparticles depends on the particle shape has been investigated in recent simulations [46,45,52,55,54,58,61,56,74]. In general, the bending energy cost for wrapping strongly depends on the shape of nanoparticles (see Section 4). The interplay of bending and adhesion energies can induce orientational changes of ellipsoidal particles relative to the membrane during wrapping [55,56]. The spontaneous wrapping depends strongly on the particle size because the adhesion energy increases with the size of a particle. The bending energy cost of wrapping, in contrast, is independent of the particle size (see Section 4). Finally, the wrapping of particles by membrane vesicles can lead to shape changes of the vesicles that lower the bending energy of the vesicles and, thus, assist the wrapping process (see Section 5).

In the next section, we start with a general discussion of the elastic and adhesive energies that are involved in the wrapping process. For nanoparticle wrapping, the dominant elastic energy is the bending energy of the membranes, which was first completely described by Wolfgang Helfrich [75].

2. Interplay of elastic and adhesive energies during wrapping

The spontaneous wrapping of particles by a membrane is governed by the interplay of the elastic energy E_{el} of the membrane and the adhesion energy E_{ad} of the particles [26,76]. The elastic energy of the membrane is the sum $E_{\mathrm{el}} = E_{\mathrm{be}} + E_{\mathrm{te}}$ of the bending energy E_{be} and the tension contribution E_{te}. The bending energy is the integral [75]

$$E_{\mathrm{be}} = \int \left[\frac{1}{2}\kappa(2M - c_o)^2 + \bar{\kappa}K\right] dA \tag{1}$$

over the membrane area A and depends (i) on the shape of the membrane, which is described by the local mean curvature M and Gaussian curvature K, and (ii) on the bending rigidity κ, modulus of Gaussian curvature $\bar{\kappa}$ and spontaneous curvature c_o as characteristic elastic properties of the membrane. The tension contribution simply is the product

$$E_{\mathrm{te}} = \sigma A \tag{2}$$

of the membrane tension σ and area A. The adhesion energy of a particle can be written as the integral

$$E_{\mathrm{ad}} = \int V(d)\, dA \tag{3}$$

over the membrane area A where $V(d)$ is the particle–membrane interaction potential, and d is the local distance of the membrane from the particle surface. The particle–membrane interaction may either result from electrostatic and Van der Waals interactions between the lipid bilayer and the particles, or may be mediated by the specific binding of receptor and ligand molecules that are anchored in the membrane and to the particle surface (see Section 7 for a more detailed discussion). The total energy that governs the wrapping process is the sum

$$E = E_{\mathrm{be}} + E_{\mathrm{te}} + E_{\mathrm{ad}} \tag{4}$$

of the elastic energy of the membrane and the adhesion energy of the particles.

The wrapping process described by the total energy in Eq. (4) depends on several length scales. These length scales are characteristic lengths (i) of the membrane, (ii) of the particles, and (iii) of the particle–membrane interaction. The characteristic length of the particle–membrane interaction is the range ρ of this interaction. Characteristic length scales of the membrane are the inverse spontaneous curvature $1/c_o$ and the 'crossover length' $\sqrt{\kappa/\sigma}$. On length scales smaller than this crossover length, the elastic energy $E_{\mathrm{el}} = E_{\mathrm{be}} + E_{\mathrm{te}}$ of the membrane is dominated by the bending energy E_{be}. On length scales larger than the crossover length, the tension contribution E_{te} dominates over the bending energy E_{be}. For membrane vesicles, an additional characteristic length is the square root of the membrane area A_p.

In this review, we focus on wrapping scenarios in which the characteristic lengths of the particles are small compared to the inverse spontaneous curvature $1/c_o$ and to the crossover length $\sqrt{\kappa/\sigma}$ of the membrane. The spontaneous curvature c_o and tension contribution E_{te} then are negligible in the elastic energy E_{el} of the membranes. These wrapping scenarios are realistic in particular for small particles with characteristic dimensions of tens of nanometers. For typical values of the bending rigidity κ between 10 and 20 k_BT [77] and a membrane tension σ of a few μN/m [78], for example, the crossover length $\sqrt{\kappa/\sigma}$ adopts values between 100 and 200 nm.

3. Wrapping of spherical particles

We first consider the wrapping of a single spherical particle of radius R by a planar membrane. One of our main points in this section and in following sections is that the range ρ of the particle–membrane interaction crucially affects the wrapping process. However, it is instructive to consider first a contact potential with a range ρ that is negligibly small compared to the particle radius R.

3.1. Contact potential with range $\rho = 0$

For a spherical particle, the minimum-energy shape of the membrane around the particle is rotationally symmetric (see Fig. 1(a)). In the case of a contact potential with potential range $\rho = 0$, the membrane shape around the particle is composed of (i) a spherical membrane segment that is bound to the particle, and (ii) an unbound catenoidal segment that smoothly connects the bound membrane to the surrounding planar membrane [26,29,30]. The bound membrane segment has a spherical shape because the contact potential requires that this segment adopts the same shape as the particle. For negligible spontaneous curvature c_o and tension σ of the membrane (see previous section), the unbound membrane adopts a catenoidal shape because the bending energy contribution of the catenoid is zero. The zero bending energy of the unbound catenoidal segments results from oppositely equal principal curvatures

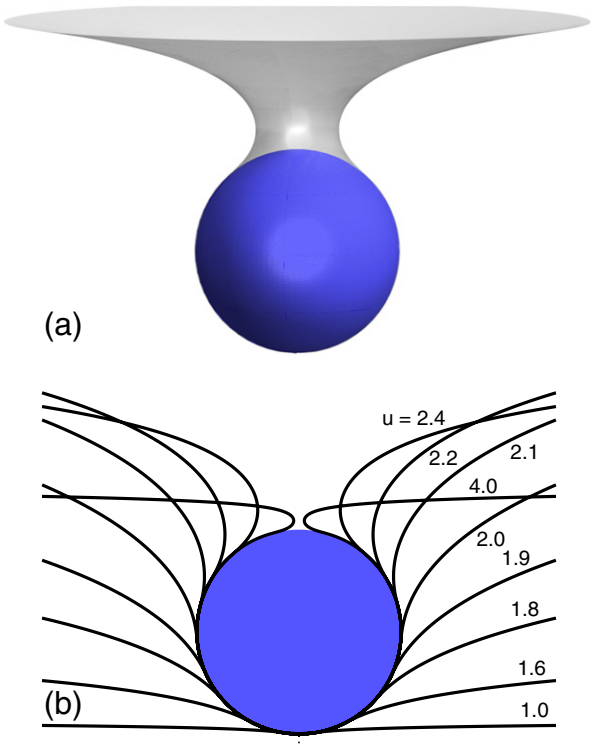

Fig. 1. (a) Minimum-energy shape of a tensionless membrane around a spherical particle with radius R for the rescaled adhesion energy $u = 2.4$ and the potential range $\rho = 0.01R$. (b) Minimum-energy profiles of the rotationally symmetric membrane shapes around a single spherical particle for the potential range $\rho = 0.01R$. The numbers indicate the values for the rescaled adhesion energy u of the different profiles [39].

$c_1 = -c_2$, which lead to a mean curvature $M = (c_1 + c_2)/2 = 0$. The mean curvature term in the bending energy in Eq. (1) thus is zero for this catenoidal segment. For shape deformations of a planar membrane considered here, the Gaussian curvature term in the bending energy is zero, too, according to the Gauss Bonnet theorem (see also below).

Since both the bending and adhesion energies of the unbound catenoidal segment are zero, the wrapping of the particle is determined by the interplay of bending and adhesion in the bound membrane segment. The mean curvature of the bound membrane is $M = 1/R$ because the principal curvatures of this spherical segment are $c_1 = c_2 = 1/R$. If this segment wraps a fraction x of the particle area $A_p = 4\pi R^2$, the bending energy $E_{be} = 2\kappa M^2 A_p x$ of the segment is

$$E_{be} = 8\pi\kappa x. \tag{5}$$

The adhesion energy of the bound membrane segment is

$$E_{ad} = -U A_p x = -4\pi R^2 U x \tag{6}$$

where $U > 0$ is the adhesion energy per area. The bending energy E_{be} is positive and opposes wrapping, while the negative adhesion energy E_{ad} favors wrapping. The total energy can be written as

$$E = E_{be} + E_{ad} = 4\pi\kappa x(2-u) \tag{7}$$

with the rescaled adhesion energy

$$u \equiv UR^2/\kappa \tag{8}$$

of the particle. For $u < 2$, the total energy E is minimal at $x = 0$, i.e. for the unbound state of the particle. For $u > 2$, the total energy is minimal for $x = 1$, i.e. for the fully wrapped state of the particle. In this fully wrapped state, the catenoidal membrane neck that connects the wrapped membrane segment to the surrounding planar membrane is infinitesimally small. As a function of u, the fraction x of the wrapped particle area thus is discontinuous at $u = 2$ (see black line in Fig. 2(a)), and the total energy is $E = 0$ for $u < 2$ and $E = 4\pi\kappa(2-u)$ for $u > 2$ (see black line in Fig. 2(b)).

3.2. Particle membrane interaction potentials with nonzero range ρ

For small particles with a characteristic size of tens of nanometers, the range ρ of the membrane–particle interaction cannot be neglected [39]. To illustrate how the interaction range ρ affects the wrapping process, we consider here a Morse interaction potential

$$V(d) = U\left(e^{-2d/\rho} - 2\, e^{-d/\rho}\right) \tag{9}$$

in which the particle–membrane attraction $V(d)$ decays exponentially with characteristic length ρ for increasing local distance d between the membrane and the particle surface. The potential $V(d)$ adopts its minimum value $-U$ at the relative distance $d = 0$, which corresponds to the equilibrium distance between a particle and a bound membrane patch in the absence of other than adhesive forces. Fig. 1(b) displays membrane profiles around a spherical particle for the potential range $\rho = 0.01R$ and various values of the rescaled adhesion energy u defined in Eq. (8). The profiles result from an energy minimization of the rotationally symmetric membrane shape around the particle [39]. In contrast to the discontinuous wrapping for $\rho = 0$, the fraction of the wrapped particle area increases continuously with u for a finite potential range ρ (see Figs. 1(b) and 2(a)). The continuous wrapping process

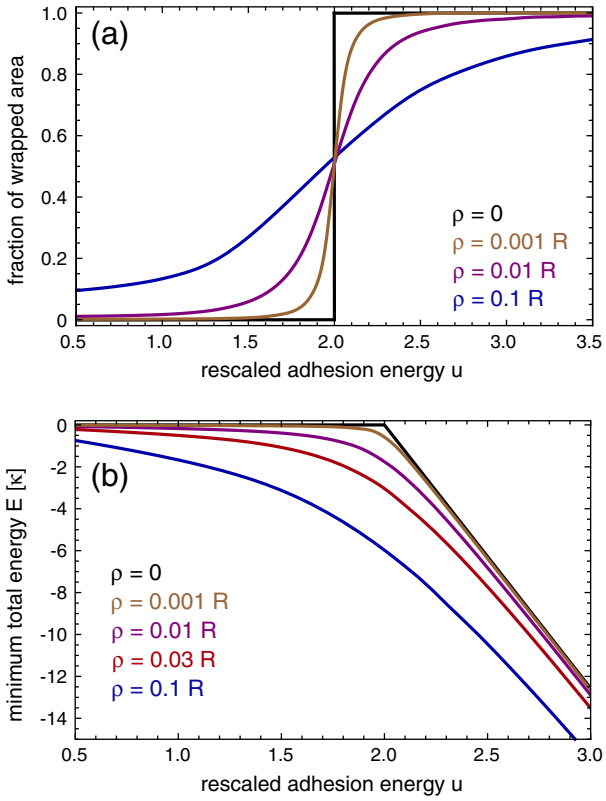

Fig. 2. (a) Area fraction of a single spherical particle with radius R that is wrapped by the membrane as a function of the rescaled adhesion energy u for different values of the potential range ρ. (b) Minimum total energy E of the membrane around a single particle as a function of the rescaled adhesion energy u for different values of the potential range ρ [39].

is centered around the value $u = 2$ of the rescaled adhesion energy at which the bending energy of the bound spherical membrane segment is oppositely equal to the adhesion energy of the segment (see above). With decreasing potential range ρ, the wrapping process becomes more abrupt and is finally discontinuous in the limit $\rho \to 0$ (see Fig. 2(a)).

In Fig. 2(b), the minimum total energy E of the membrane is shown as a function of the rescaled adhesion energy u for different values of the potential range ρ. The minimum energy E is negative for $\rho > 0$ and decreases both with increasing rescaled adhesion energy u and increasing potential range ρ. The decrease of E with increasing potential range ρ results from a favorable interplay of bending and adhesion energies in the contact region in which the membrane detaches from the particle [39]. The contact region connects the bound spherical membrane segment and the unbound catenoidal segment. In this contact region, the membrane already approaches the catenoidal shape of the unbound membrane segment with zero bending energy but still gains adhesion energy due to the finite potential range ρ. With increasing potential range ρ, the minimum energy E decreases because the contact region of the membrane becomes wider.

Full membrane crossing of the particle eventually requires a breaking of the catenoidal membrane neck through a fission process. The breaking of the membrane neck changes the topology of the membrane and leads to an additional energy change $\Delta E = 4\pi\bar{\kappa}$ that results from the Gaussian curvature term in the bending energy in Eq. (1). Because of the Gauss Bonnet theorem of differential geometry, this energy change does not depend on the particle shape. The Gauss Bonnet theorem implies that all membrane shapes that result from deformations of a sphere lead to the same integral $\int K\,dA = 4\pi$ of the Gaussian curvature K as the sphere. Similarly, all local deformations of a planar membrane lead to the same integral $\int K\,dA = 0$ of a planar surface.

The breaking of the catenoidal membrane neck required for full particle crossing can only occur if this neck is sufficiently small so that the apposing membrane surfaces in the neck are close. For a finite potential range ρ, the neck is small if the rescaled adhesion energy u is sufficiently large such that the particle is nearly fully wrapped by the membrane (see Fig. 1(b)). As illustrated in Fig. 2(a), an increase in the potential range ρ requires larger values of the rescaled adhesion energy u for full wrapping and subsequent membrane crossing.

4. Wrapping of non-spherical particles

4.1. Full wrapping of ellipsoidal particles

The wrapping of particles by a membrane depends on the shape of these particles. We investigate here first the bending energy cost for full wrapping in the case of a contact potential with range $\rho = 0$. For such a potential, the shape of the membrane around the particle is identical to the particle shape. As model particles, we will consider ellipsoidal particles.

The shape of ellipsoidal particles can be described by the parametrization

$$\begin{pmatrix} x(\theta,\phi) \\ y(\theta,\phi) \\ z(\theta,\phi) \end{pmatrix} = \begin{pmatrix} a\sin\theta\cos\phi \\ a\sin\theta\sin\phi \\ b\cos\theta \end{pmatrix} \tag{10}$$

with $0 \le \theta \le \pi$ and $0 \le \phi \le 2\pi$ and the two characteristic lengths a and b of the particles. In this parametrization, the particles are rotationally symmetric around the z-axis. The shape of the particles can be characterized by the aspect ratio

$$r = b/a. \tag{11}$$

The particles have an oblate shape for $r < 1$, and a prolate shape for $r > 1$ (see Fig. 3). For $r = 1$, the particles are spherical and have the radius $R = a = b$.

The mean curvature of the wrapped membrane depends on the angle θ of the parametrization in Eq. (10) and can be written as

$$M(\theta) = \frac{r\left(3 + r^2 - \left(r^2-1\right)\cos 2\theta\right)}{\sqrt{2}a\left(1 + r^2 - \left(r^2-1\right)\cos 2\theta\right)^{3/2}}. \tag{12}$$

In this parametrization, area elements of the membrane can be expressed as $dA = f(\theta)\mathrm{d}\theta\,\mathrm{d}\phi$ with

$$f(\theta) = \frac{a^2}{\sqrt{2}}\left(1 + r^2 - \left(r^2-1\right)\cos 2\theta\right)^{1/2}\sin\theta. \tag{13}$$

The bending energy of the membrane wrapped around the ellipsoidal particle then is

$$E_{\mathrm{be}}(r) = 2\kappa\int_0^{\pi} M(\theta)^2 f(\theta) 2\pi\,\mathrm{d}\theta \tag{14}$$

$$= \frac{2\pi\kappa}{3}\left(7 + \frac{2}{r^2} + \frac{3r^2\,\mathrm{arctanh}\left(\sqrt{1-r^2}\right)}{\sqrt{1-r^2}}\right). \tag{15}$$

For small and large aspect ratios r, respectively, this exact expression for the bending energy can be approximated as

$$E_{\mathrm{be}}(r) \simeq \pi\kappa\left(\frac{8}{3} + \pi r\right) \qquad \text{for } r \gg 1 \tag{16}$$

$$E_{\mathrm{be}}(r) \simeq \frac{2\pi\kappa}{3}\left(7 + \frac{2}{r^2}\right) \qquad \text{for } r \ll 1. \tag{17}$$

The bending energy of the wrapped membrane only depends on the aspect ratio r of the ellipsoidal particles, but not on the particle size. In other words, increasing (or decreasing) both characteristic lengths a and b of the particles by the same factor does not change the bending energy. This 'scale invariance' of the bending energy results from the fact that an increase in the particle area is compensated by a decrease in the mean curvature. For a spherical particle with aspect ratio $r = 1$ for example, the particle area and mean curvature are $A_P = 4\pi R^2$ and $M = 1/R$, which leads to the bending energy $E_{\mathrm{be}} = 2\kappa M^2 A_P = 8\pi\kappa$ that does not depend on the particle radius $R = a = b$ (see also previous section).

The bending energy $E_{\mathrm{be}}(r)$ is minimal for the aspect ratio $r = 1$ of spherical particles, and increases both with increasing and decreasing aspect ratio r (see Fig. 4(a) and Eqs. (16) and (17)). Therefore, a

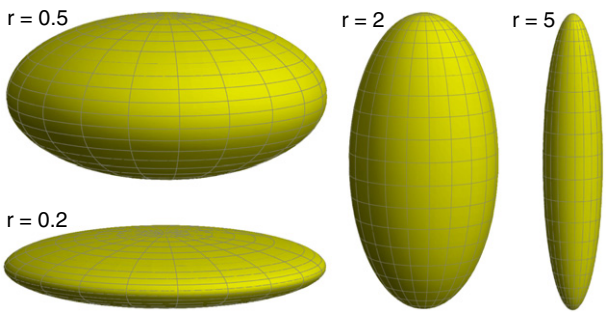

Fig. 3. Ellipsoidal particles with different aspect ratios r. The particles have an oblate shape for $r < 1$, and a prolate shape for $r > 1$.

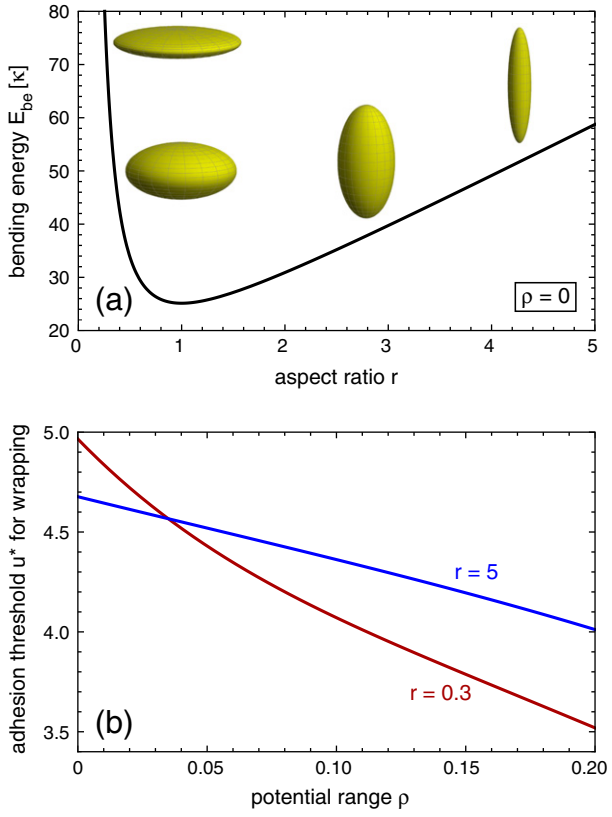

Fig. 4. (a) Bending energy E_{be} of the membrane wrapped around an ellipsoidal particle as a function of the particle's aspect ratio r for the range $\rho = 0$ of the particle–membrane interaction. For this interaction range, the wrapped membrane adopts the same shape as the particle. The bending energy $E_{be}(r)$ is given in Eq. (15). (b) Threshold value u^* of the rescaled adhesion energy $u = UR^2/\kappa$ for the full wrapping of ellipsoidal particles with area $4\pi R^2$ and aspect ratio $r = 0.3$ and 5, respectively, as a function of the range ρ of the particle–membrane interaction in Eq. (9). At the threshold value u^*, the total energy E obtained from numerical minimization vanishes.

spherical particle requires smaller adhesion energies for full wrapping than an ellipsoidal particle if these particles have the same area. The threshold value of the adhesion energy for full wrapping can be determined from the total energy

$$E = E_{be}(r) + E_{ad} = E_{be}(r) - A_P U. \tag{18}$$

For ellipsoidal particles with the same area $A_P = 4\pi R^2$ as spherical particles of radius R, the threshold value of the rescaled adhesion energy u defined in Eq. (8) is

$$u^* = E_{be}(r)/(4\pi\kappa). \tag{19}$$

At this threshold value of u, the total energy E is 0, i.e. the adhesion energy E_{ad} favoring wrapping is oppositely equal to the bending energy cost $E_{be}(r)$. As in the previous section, we have assumed here that the membrane wrapping the particle is still connected via an infinitesimally small neck to a surrounding membrane. The Gaussian curvature term in the bending energy in Eq. (1) then does not affect the wrapping process.

So far, we have focused on a contact potential with range $\rho = 0$ for which the wrapped membrane has the same shape as the particle. For a finite potential range ρ, the total energy can be determined via numerical minimization. We find that the adhesion threshold value u^* for full wrapping decreases with ρ (see Fig. 4(b)). This decrease results from deviations between the membrane shape and the particle shape in regions of high surface curvature of the particle, which reduce the bending energy cost for full wrapping.

4.2. Orientational changes of ellipsoidal particles during wrapping

In the previous subsection, we have considered the bending energy cost and adhesion energy threshold for the full wrapping of ellipsoidal particles. During the wrapping process from partial to full wrapping of ellipsoidal particles, the interplay of bending and adhesion energies can lead to orientational changes of the particles relative to the membrane [55,56]. Fig. 5 illustrates results for the wrapping of a prolate particle by a vesicle membrane obtained from Monte Carlo minimization [55]. In the Monte Carlo simulations, the fraction x of the particle area that is wrapped by the vesicle membrane is constrained by harmonic potentials, and the bending energy of the vesicle is minimized via simulated annealing [79]. The volume of the vesicle is free to adjust in the simulations, which corresponds to experimental situations in which osmotically active particles are absent (see next section). For partially wrapped states of the prolate particle with wrapped area fractions x smaller than about 0.63, the particle is oriented with its side towards the vesicle because the bending energy of the vesicle is minimal in this orientation. For nearly fully wrapped states with larger values of x, the prolate particle is oriented with its tip towards the vesicle.

These orientational changes can be understood from the different bending energy cost for the wrapping of the sides and tips of ellipsoidal particles. At the side of the ellipsoidal particles, the mean curvature obtained from Eq. (12) is

$$M(\theta = \pi/2) = \frac{1 + r^2}{2ar^2}. \tag{20}$$

At the tip of the particles, the mean curvature is

$$M(\theta = 0) = \frac{r}{a}. \tag{21}$$

For prolate particles with aspect ratio $r > 1$, the mean curvature at the tip exceeds the mean curvature at the side of the particle. For large r, the mean curvature at the side tends towards the value $1/2a$, which is independent of the aspect ratio r. In contrast, the mean curvature at the tip increases proportionally to r. For partially wrapped states of a prolate particle in which the membrane adheres to a small fraction x

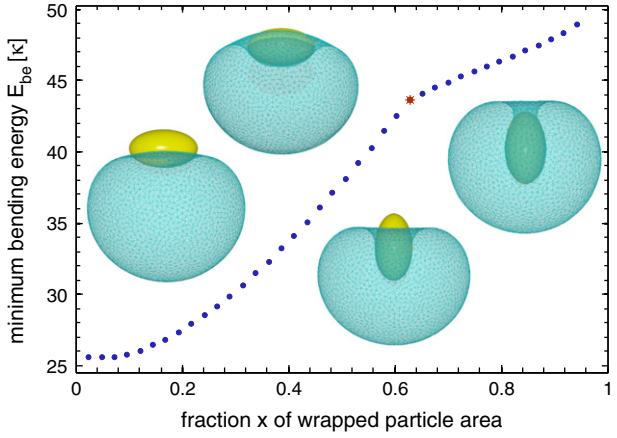

Fig. 5. Minimum bending energy of a triangulated vesicle obtained from Monte Carlo minimization as a function of the wrapped area fraction x of a prolate particle with aspect ratio 1.8. The particle changes its orientation during wrapping [55]. The particle is oriented with its side towards the vesicle center if the wrapped area fraction x is smaller than about 0.63 (see Monte Carlo snapshots on top left for $x = 0.35$ and 0.6). For wrapped area fractions larger than about 0.63 (red star), the particle is oriented with its tip towards the vesicle center (see Monte Carlo snapshots on bottom right for $x = 0.67$ and 0.91). The volume of the vesicle is free to adjust in the Monte Carlo simulations, which corresponds to experimental situations in which osmotically active particles are absent (see Section 5).

of the particle area, the bending energy cost for adhesion at the side of the particle as in the two upper left Monte Carlo snapshots of Fig. 5 therefore is smaller than at the tips. In contrast, for nearly fully wrapped states with wrapped area fractions x close to 1, it is energetically favorable to 'leave out' at least one of the two tips of the prolate particle from wrapping as in the two lower right Monte Carlo snapshots of Fig. 5 in which the particle is oriented with one of its two tips towards the vesicle membrane.

For oblate particles with aspect ratio $r < 1$, the mean curvature at the tips is smaller than at the sides. In partially wrapped states, an orientation of oblate particles with its tip towards the membrane therefore is energetically favorable and has been observed in Monte Carlo simulations [55] and numerical minimizations [56]. In nearly fully wrapped states, in contrast, the bending energy cost for wrapping is smaller if the oblate particle is oriented with its more strongly curved side towards the membrane.

The higher bending energy cost for more strongly curved regions of nonspherical particles also stabilizes partially wrapped states of such particles in which parts of these strongly curved regions, e.g. one of the tips of a prolate particle, are not wrapped by the membrane [54,56].

5. Internalization of particles by vesicles

5.1. Presence of osmotically active particles

In the previous sections, we have considered the interplay of bending and adhesion in membrane segments that are wrapped around particles. However, we have neglected any global changes in the shape and bending energy of the surrounding membrane during wrapping. Such changes occur during the wrapping and internalization of particles by a vesicle if the solvent inside and outside the vesicle contains osmotically active molecules such as salts or sugars that cannot cross the membranes [32,38]. Since water can cross the membranes, the vesicles then 'adjust' their volume V so that the osmotic pressure vanishes. The shape and bending energy of such vesicles depend on their area-to-volume ratio [80,81], which can be characterized by the reduced volume

$$v = 6\sqrt{\pi}V/A^{3/2} \le 1. \tag{22}$$

The maximal value $v = 1$ of the reduced volume corresponds to the area-to-volume ratio of a sphere. The area A of vesicles can be taken to be constant because of the near incompressibility of lipid membranes.

Fig. 6(a) illustrates how the shape and bending energy of the vesicles depend on the reduced volume for a negligible spontaneous curvature c_o of the vesicle membrane [81]. The bending energy decreases with the reduced volume v and attains the minimum value $8\pi\kappa$ for spherical vesicles with $v = 1$. For small reduced volumes v, the vesicle adopts a stomatocyte shape with bending energy $16\pi\kappa$ in the limit $v \to 0$. In this limit, the stomatocyte shape consists of two spheres with bending energy $8\pi\kappa$ each, which are connected by a neck of negligible bending energy.

During the internalization of a particle, a vesicle with constant area A and volume V changes its shape and becomes 'more spherical', because the membrane wrapped around the particle effectively 'decreases' the area of the vesicle membrane, and the volume of the particle inside the vesicle 'increases' the volume of the vesicle. The effective reduced volume of the vesicle after internalization of a particle with volume V_P and surface area A_P thus is

$$v_{\rm ef} = 6\sqrt{\pi}\frac{V + V_P}{(A - A_P)^{3/2}}. \tag{23}$$

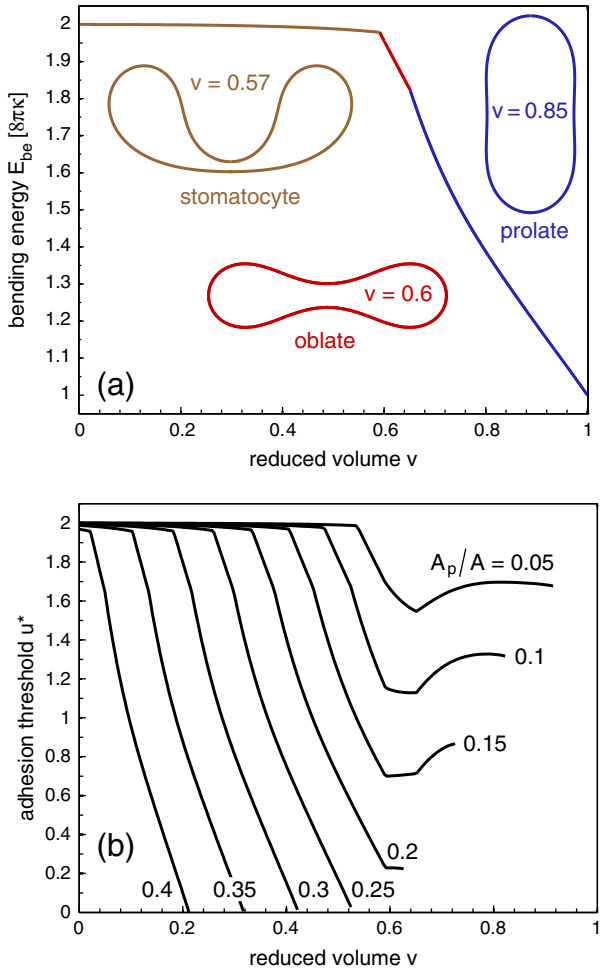

Fig. 6. (a) Minimum bending energy E_{be} of vesicle as a function of the reduced volume v for negligible spontaneous curvature c_o of the vesicle membrane. The vesicle adopts a stomatocyte shape for small values of v (brown), an oblate shape for intermediate values of v (red), and a prolate shape for large v. (b) Adhesion threshold u^* for full wrapping of a spherical particle as a function of the initial reduced volume v of the vesicle for different ratios A_P/A of the particle area A_P and vesicle area A. The change in the shape and bending energy of the vesicle strongly reduces the threshold value u^* of the rescaled adhesion energy.

For a spherical particle, we have $V_p = A_p^{3/2}/(6\sqrt{\pi})$ and therefore

$$v_{\rm ef} = \frac{v + (A_P/A)^{3/2}}{(1 - A_P/A)^{3/2}}. \tag{24}$$

For such a spherical particle, the effective volume $v_{\rm ef}$ of the vesicle only depends on its initial reduced volume v and the ratio A_P/A of the particle area and vesicle area.

Since the effective reduced volume $v_{\rm ef}$ of a vesicle after internalization of a particle is larger than its initial reduced volume v, the bending energy of the vesicle decreases during internalization. This decrease in the bending of the vesicle reduces the adhesion threshold value u^* for full wrapping (see Fig. 6(b)). The threshold value u^* of the rescaled adhesion energy u of spherical particles defined in Eq. (8) can be calculated from the energy difference

$$\Delta E = E_{\rm be}^{(\rm pa)} - UA_P + E_{\rm be}^{(\rm ve)}(v_{\rm ef}) - E_{\rm be}^{(\rm ve)}(v) \tag{25}$$

before and after internalization. Here, $E_{\rm be}^{(\rm pa)}$ denotes the bending energy of the membrane wrapped around the particle, and $E_{\rm be}^{(\rm ve)}$ is the bending energy of the (remaining) vesicle membrane. At $u = u^*$, the energy difference ΔE vanishes. We have assumed here that the membrane

wrapped around the particle is still connected to the vesicle membrane by a small catenoidal membrane neck of zero bending energy. Breaking this neck for full internalization leads to an additional energy term $4\pi\bar{\kappa}$ in Eq. (25) that results from the Gaussian curvature term in the bending energy in Eq. (1) (see Section 3).

In Fig. 6(b), the adhesion threshold u^* of a spherical particle is shown as a function of the initial reduced volume v of the vesicle for several values of the ratio A_P/A of the particle area A_P and vesicle area A. The particles can only be fully wrapped by the vesicle if the initial reduced volume v of the vesicle is sufficiently low. The curves in Fig. 6(b) therefore end at the maximal value

$$v^{\max} = (1-A_P/A)^{3/2} - (A_P/A)^{3/2} \tag{26}$$

of v for which the effective reduced volume v_{ef} after internalization is equal to 1. For area ratios A_P/A larger than about 0.25, the bending energy change of the vesicle can reduce the adhesion threshold u^* to values close to 0 (see Fig. 6(b)). The reason for this large reduction is that the maximal possible bending energy change of the vesicle is $-8\pi\kappa$ for a change of the reduced volume from $v = 0$ to $v_{ef} = 1$ (see Fig. 6(a)), which compensates the bending energy cost $E_{be}^{(pa)} = 8\pi\kappa$ for wrapping the spherical particle.

5.2. Absence of osmotically active particles

In the absence of osmotically active particles such as salts or sugars, a vesicle can freely adjust its volume. Since the spherical shape has the lowest bending energy (see Fig. 6(a)), the vesicle adopts this shape before and after the internalization of particles. The bending energy $E_{be}^{(ve)}$ of the vesicle introduced in Eq. (25) thus does not change during internalization. The adhesion threshold of the particles then has the same value as for planar membranes. For adhesion energies beyond this threshold, the vesicle fills up with internalized particles (see Fig. 7). The maximum number of particles that can be internalized by a vesicle depends on the area A of the vesicle membrane and on the area A_P and volume V_P of the particles. This maximum number follows from the equation

$$\frac{N_{\max} V_p}{f} = \frac{\left(A - A_p N_{\max}\right)^{3/2}}{6\sqrt{\pi}} \tag{27}$$

where f is the volume fraction for close packing of the particles. For spherical particles, for example, we have $f = \pi/3\sqrt{2}$. The left-hand side of Eq. (27) is the volume of the $N_{\max}$ densely packed particles that fill up the vesicle, and the right-hand side of Eq. (27) is the volume of a spherical vesicle with area $A - N_{\max}A_p$, i.e. with the membrane area that remains after wrapping $N_{\max}$ particles of area A_P. Eq. (27) can be rewritten as

$$A = A_P N_{\max} + \left(6\sqrt{\pi}V_P/f\right)^{2/3} N_{\max}^{2/3}. \tag{28}$$

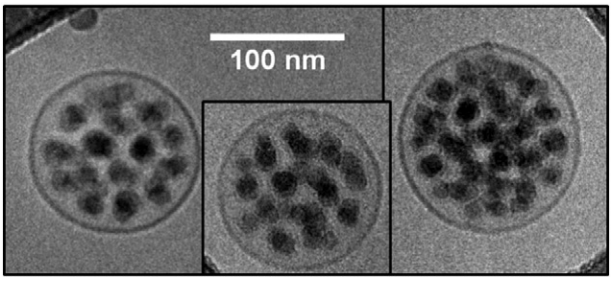

Fig. 7. Micrographs of cryo-transmission electron microscopy of SiO^2 nanoparticles (Ludox, 16 nm diameter, 0.05 wt.%) wrapped and internalized by DOPC vesicles (0.1 wt.%) in aqueous solution [82,83].

For large $N_{\max}$, i.e. for a small area ratio A_P/A, the first term on the right-hand side proportional to $N_{\max}$ dominates over the second term, which leads to

$$N_{\max} \simeq A/A_P. \tag{29}$$

6. Cooperative wrapping of nanoparticles

In the previous sections, we have considered the wrapping of individual nanoparticles by membranes. Recent simulations indicate the cooperative wrapping of several nanoparticles in tubular membrane structures [48,50,53]. Fig. 8 illustrates results from Monte Carlo minimization of triangulated vesicles in contact with two nanoparticles [48]. In these simulations, the extent to which the particles can be wrapped by the vesicle membrane is controlled by the reduced volume v defined in Eq. (22). For large values of v, adhesive particles can only be partially wrapped by the vesicle membrane. For such large values, the Monte Carlo simulations indicate bound states in which two particles are equally wrapped by the vesicle as in Fig. 8(a). For smaller values of v, the simulations indicate more strongly bound states in which the two particles are jointly wrapped by a membrane tube that invaginates into the vesicle, see Fig. 8(b).

In Fig. 8(c), the minimum total energy E of a vesicle with two adsorbed particles is displayed as a function of the particle distance r.

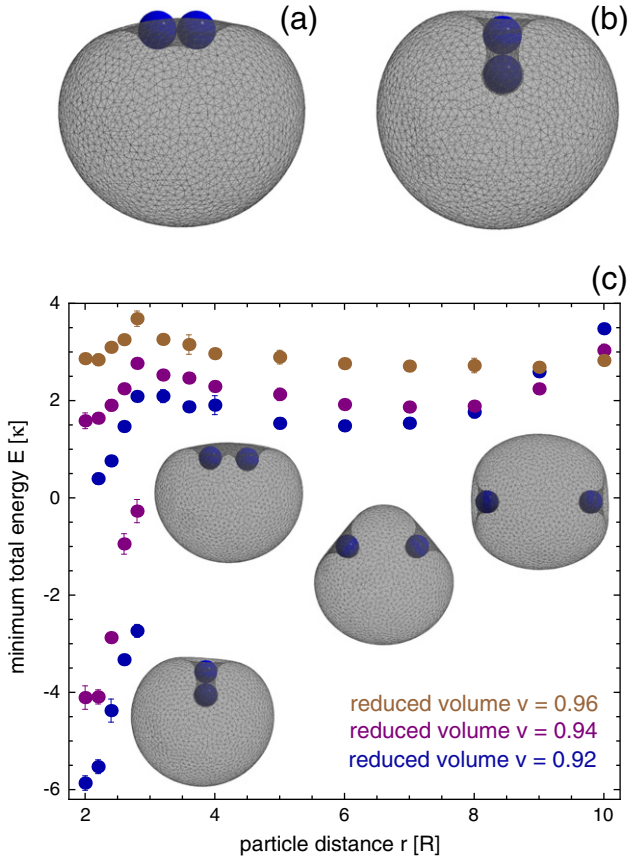

Fig. 8. (a) Bound minimum-energy state of two particles for the reduced volume $v = 0.96$ of the vesicle and the rescaled adhesion energy $u \equiv UR^2/\kappa = 2$ of the particle where U is the adhesion energy per area, R is the particle radius, and κ is the bending rigidity of the vesicle membrane. (b) Bound minimum-energy state of two particles for $v = 0.92$ and $u = 2.33$. (c) Total energy E of a vesicle with two adsorbed particles as a function of the particle distance r for the rescaled adhesion energy $u = 2.33$ and the values $v = 0.92$, 0.94, and 0.96 of the reduced volume [48]. The particles with radius R are in contact at the distance $r = 2R$. The four snapshots represent minimum energy conformations for the reduced volume $v = 0.92$ at particle distances with $r/R = 2$, 3.2, 6 and 9.

This energy is obtained from minimization via Monte Carlo simulated annealing for a fixed distance r of the particles. At the reduced volume $v = 0.93$, the total energy $E(r)$ exhibits local minima at the contact distance $r = 2R$ of the particles and at a distance r between $6R$ and $9R$, separated by an energy barrier. The local minimum of E at the contact distance $r = 2R$ corresponds to the bound state of the particles shown in Fig. 8(a) in which both particles are symmetrically wrapped by the vesicle membrane. At the reduced volume $v = 0.92$ and 0.94, there are additional branches of low-energy conformations with negative values of E at distances $r < 3R$ of the particles. In these low-energy conformations, the particles are jointly but asymmetrically wrapped by a membrane tube that invaginates into the vesicles (see Fig. 8(b) and snapshot at bottom left of Fig. 8(c)). In these conformations, the wrapping of the particles is asymmetric since the particle at the tip of the invagination is more strongly wrapped. Besides these low-energy conformations, there are branches of higher-energy conformations with positive values of E in which the particles are symmetrically wrapped as in Fig. 8(a). In the simulations, the particle–membrane interaction is modeled by a square-well potential with depth U and width $0.1R$.

The particle-filled membrane tubes form because of an energy gain for the cooperative wrapping of nanoparticles in tubes, compared to the individual wrapping of the particles. This energy gain can be calculated by minimizing the energies of the rotationally symmetric shapes of membrane tubes and of membrane segments wrapping single particles [39]. Fig. 9(a) illustrates the three-dimensional shape of a two-particle tube protruding from a planar membrane, and Fig. 9(b) and (c) display the shape and profiles of the membrane around three central particles of a long tube. The membrane shape around the central particles of such long tubes is periodic along the axis of rotation, and consists of spherical segments bound to the particles that are connected by unbound catenoidal membrane segments between the particles of zero bending energy. The total energy of these tubes is minimized with respect to the distance L of neighboring particles, which depends both on the rescaled adhesion energy u defined in Eq. (8) and on the range ρ of the adhesion potential in Eq. (9) (see Fig. 10(a)).

The energy gain per particle for the cooperative wrapping in long tubes can be defined as

$$\Delta E = E_{\text{tube}} - E_{1\text{p}} \tag{30}$$

where E_{tube} is the minimum total energy for a central particle in the tubes, and $E_{1\text{p}}$ is the minimum total energy of a single wrapped particle shown in Fig. 2(b). In Fig. 10(b), the energy difference ΔE is displayed as a function of the rescaled adhesion energy u for different values of the potential range ρ. The energy difference ΔE is negative for rescaled

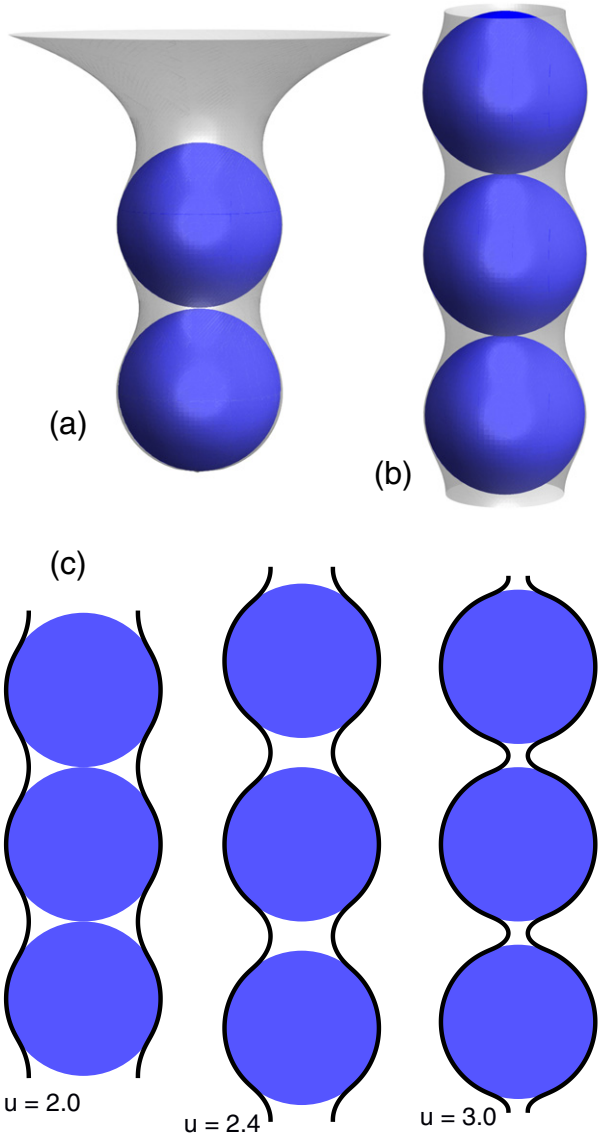

Fig. 9. Minimum-energy states of (a) two particles wrapped in a membrane tube and (b) three central particles of a long membrane tube for the range $\rho = 0.1R$ of the particle–membrane adhesion potential and the rescaled adhesion energy $u = UR^2/\kappa = 3$ where R is the particle radius and κ is the bending rigidity of the membrane. (c) Minimum-energy membrane profiles around three central particles of a long tubule for the potential range $\rho = 0.01R$ and different rescaled adhesion energies u. The particle–membrane interaction here is described by the adhesion potential (9) [39].

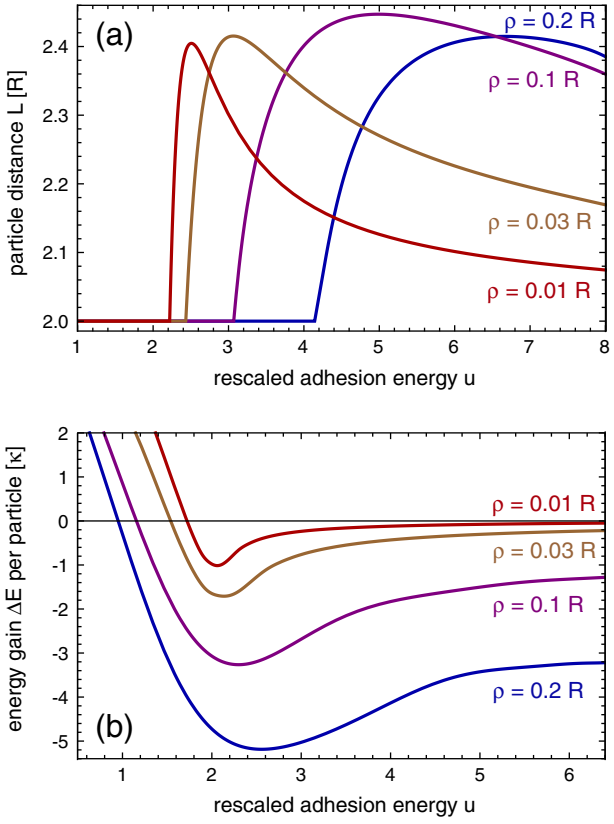

Fig. 10. (a) Distance $L \geq 2R$ of neighboring particles in the tube at which the total energy is minimal, and (b) energy gain ΔE per particle for the cooperative wrapping in long tubes defined in Eq. (**30**) as a function of the rescaled adhesion energy u for various values of the potential range ρ [39].

adhesion energies u larger than a value u_0. These negative values of ΔE indicate an energy gain for the cooperative wrapping in tubes. The value u_0 with $\Delta E = 0$ is located between $u = 1.0$ and $u = 2.0$ and, thus, at values at which single particles are less than half wrapped (see Fig. 2(a)). For a given potential range ρ, the energy difference ΔE adopts a minimum value at rescaled adhesion energies between $u = 2.0$ and $u = 3.0$.

The energy difference ΔE between cooperative wrapping and individual wrapping strongly depends on the potential range ρ. The minimum values of the energy difference ΔE per particle are -5.2κ for $\rho = 0.2R$, -3.3κ for $\rho = 0.1R$, -1.7κ for $\rho = 0.03R$, and -1.0κ for $\rho = 0.01R$. Since typical values of the bending rigidity κ range from 10 k_BT to 20 k_BT, these minimum values of ΔE are large compared to the thermal energy k_BT. The absolute value of the energy difference ΔE decreases for intermediate values of the rescaled adhesion energies u between 3.0 and 6.0. However, at the large rescaled adhesion energy $u = 6.0$, the energy differences $\Delta E = -3.2\kappa$, -1.3κ, and -0.24κ for the potential ranges $\rho = 0.2R$, $0.1R$, and $0.03R$ are still large in magnitude compared to k_BT for typical values of κ. These values for the energy difference ΔE have been obtained for the particle–membrane interaction in Eq. (9). In simulations, stable particle-filled membrane tubes have been observed for square-well potentials [48], for van der Waals potentials [50], and for specific interactions mediated by membrane-anchored receptors and ligands and, thus, for rather diverse particle–membrane interactions [53].

The energy gain for the cooperative wrapping results from a favorable interplay between bending and adhesion energies in the contact regions in which the membrane detaches from the particles [39]. The cooperative wrapping in tubes simply is favorable because a central particle in a tube has two such contact regions with the membrane, while a single wrapped particle only has one contact region. The energy gain depends on the potential range ρ because the interplay between bending and adhesion becomes more pronounced with increasing ρ.

The large energy gain for the cooperative wrapping of particles implies strongly attractive elastic interactions between the adhering spherical particles that are mediated by the membrane. These elastic interactions result from the fact that the minimum total energy of two or more adhering particles depends on the particle distances. At the optimal distance L for the cooperative wrapping of the particles by membrane tubes, the total energy is significantly lower than at large distances at which the particles are wrapped individually by the membrane (see Fig. 10). Such elastic interactions have been previously studied for membrane inclusions that locally deform the membranes [84–87], and for adsorbed rodlike particles with parallel orientation [88,89]. These elastic interactions are repulsive for rotationally symmetric and equally oriented membrane inclusions and for rodlike particles that adsorb to the same side of the membrane. In contrast, the elastic interactions for the cooperative wrapping of spherical nanoparticles by membrane tubes are strongly attractive. Membrane shape fluctuations can induce additional attractive interactions between adsorbed particles since the particles suppress such fluctuations in their adhesion zones. However, these fluctuation-induced, entropic interactions are of the order of the thermal energy k_BT [84,90–92] and thus significantly weaker than the elastic energy gain ΔE for the cooperative wrapping (see Fig. 10(b)).

In experiments, the aggregation of nanoparticles in solution is typically prevented by repulsive interactions between the nanoparticles, e.g. by electrostatic interactions if the particles are charged. In general, such repulsive interactions can affect the energies of the particle-filled membrane tubes, in particular if neighboring particles in these tubes are in contact. For simplicity, the nanoparticles considered in the calculations and simulations of Figs. 8 to 10 exhibit only repulsive hard-sphere interactions. However, it is important to note that the neighboring particles in membrane tubes are not in contact at intermediate and large values of the rescaled adhesion energy u (see Figs. 9(c) and 10(a)). For such rescaled adhesion energies, repulsive interactions between the particles only play a role if their interaction range is larger than the distance between the surfaces of neighboring particles in the tubes.

7. Discussion

The wrapping of single particles and the cooperative wrapping of nanoparticles in membrane tubes are strongly affected by the range of the particle–membrane adhesion potential (see Sections 3 and 6). This range depends on the interactions that mediate adhesion, which are either 'generic' interactions between the lipid bilayer of the membrane and the particle [17,19,93,20], or 'specific' interactions between receptor and ligand proteins or other adhesion molecules that are anchored to the membrane and the particle surface [18,66]. Generic interactions that can lead to adhesion are electrostatic interactions if the membranes and particle surfaces are oppositely charged, or van der Waals forces. In the presence of salt, the range of electrostatic interactions can be quantified by the Debye screening length. Partial wrapping of charged nanoparticles by vesicles can lead to emulsions of 'decorated' vesicles that are stabilized by the electrostatic repulsion between the nanoparticles [94–97]. In general, the strength of generic interactions between membranes and surfaces is modulated by an entropic repulsion from membrane shape fluctuations [98,99]. In biological systems, the generic interactions of nanoparticles and membranes are altered by a 'corona' of proteins adsorbed on the particles [100,101].

The specific adhesion of nanoparticles to membranes can be described by an effective adhesion potential if the adhesion is mediated by a relatively large number of receptor-ligand bonds [102]. The effective adhesion energy depends on the concentrations and the binding free energy of the receptor and ligand molecules, while the range of the effective adhesion potential is determined by membrane anchoring, length, and flexibility of these molecules [102,103].

Both for generic and specific adhesion, typical values for the range of the particle–membrane interaction are of the order of one nanometer. For nanoparticles with characteristic dimensions of tens of nanometers, such values for the interaction range are a few percent of the particle dimension. These interaction ranges strongly affect the wrapping of single particles (see Fig. 2) and lead to a large energy gain for the cooperative wrapping of nanoparticles in membrane tubes (see Fig. 10(b)).

In this review, we have focused on elastic models of membranes that capture the interplay of bending and adhesion energies during wrapping. Molecular simulations can provide further insights on the interactions of nanoparticles and membranes, in particular for small particles with characteristic lengths that are comparable to the membrane thickness (see Fig. 11 for an example), and for particles that penetrate into the membrane bilayer [104,44,59].

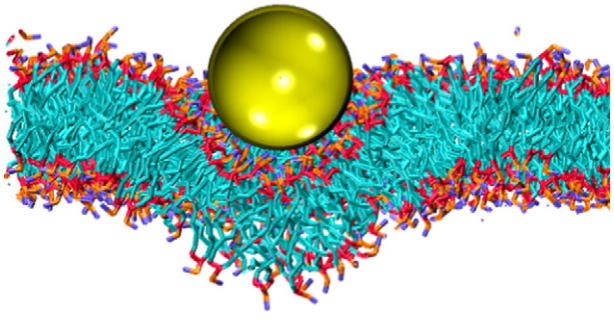

Fig. 11. Snapshot from a discrete molecular dynamics (DMD) simulation of a nanoparticle interacting with a DPPC bilayer membrane [105]. The color scheme is: purple (DPPC choline entity), orange (DPPC phosphate group), red (DPPC ester groups), cyan (DPPC alkyl tail groups), yellow (nanoparticle). In DMD simulations, particles interact via a combination of hard-sphere and square-well potentials, which means that the forces on particles only need to be calculated when discontinuities in the potentials are encountered. This allows for faster simulations than traditional molecular dynamics, enabling examination of larger membrane systems and longer time scales [106].

Acknowledgments

Financial support from the Deutsche Forschungsgemeinschaft (DFG) via the International Research Training Group 1524 "Self-Assembled Soft Matter Nano-Structures at Interfaces" is gratefully acknowledged.

References

[1] Nel AE, Mädler L, Velegol D, Xia T, Hoek EMV, Somasundaran P, et al. Understanding biophysicochemical interactions at the nano-bio interface. Nat Mater 2009;8:543–57.
[2] Barbe C, Bartlett J, Kong L, Finnie K, Lin H, Larkin M, et al. Silica particles: a novel drug-delivery system. Adv Mater 2004;16:1959–66.
[3] De Jong WH, Borm PJA. Drug delivery and nanoparticles: applications and hazards. Int J Nanomedicine 2008;3:133–49.
[4] Davis ME, Chen ZG, Shin DM. Nanoparticle therapeutics: an emerging treatment modality for cancer. Nat Rev Drug Discov 2008;7(9):771–82.
[5] Petros RA, DeSimone JM. Strategies in the design of nanoparticles for therapeutic applications. Nat Rev Drug Discov 2010;9(8):615–27.
[6] Wu S-H, Hung Y, Mou C-Y. Mesoporous silica nanoparticles as nanocarriers. Chem Commun (Camb) 2011;47(36):9972–85.
[7] Project on emerging nanotechnologies. Consumer products inventory. Retrieved [date accessed], from http://www.nanotechproject.org/cpi; 2013.
[8] Oberdörster G, Oberdörster E, Oberdörster J. Nanotoxicology: an emerging discipline evolving from studies of ultrafine particles. Environ Health Perspect 2005;113(7):823–39.
[9] Leroueil PR, Hong S, Mecke A, Baker J, James R, Orr BG, et al. Nanoparticle interaction with biological membranes: does nanotechnology present a Janus face? Acc Chem Res 2007;40:335–42.
[10] Marquis BJ, Love SA, Braun KL, Haynes CL. Analytical methods to assess nanoparticle toxicity. Analyst 2009;134:425–39.
[11] Winnik FM, Maysinger D. Quantum dot cytotoxicity and ways to reduce it. Acc Chem Res 2013;46(3):672–80.
[12] Lu X, Liu Y, Kong X, Lobie PE, Chen C, Zhu T. Nanotoxicity: a growing need for study in the endocrine system. Small 2013;9(9–10):1654–71.
[13] Mukherjee S, Ghosh RN, Maxfield FR. Endocytosis. Physiol Rev 1997;77:759–803.
[14] Conner S, Schmid S. Regulated portals of entry into the cell. Nature 2003;422:37–44.
[15] Hurley JH, Boura E, Carlson L-A, Różycki B. Membrane budding. Cell 2010;143:875–87.
[16] Rodriguez PL, Harada T, Christian DA, Pantano DA, Tsai RK, Discher DE. Minimal"self" peptides that inhibit phagocytic clearance and enhance delivery of nanoparticles. Science 2013;339:971–5.
[17] Dietrich C, Angelova M, Pouligny B. Adhesion of latex spheres to giant phospholipid vesicles: statics and dynamics. J Phys II 1997;7:1651–82.
[18] Koltover I, Rädler J, Safinya C. Membrane mediated attraction and ordered aggregation of colloidal particles bound to giant phospholipid vesicles. Phys Rev Lett 1999;82:1991–4.
[19] Fery A, Moya S, Puech P, Brochard-Wyart F, Möhwald H. Interaction of polyelectrolyte coated beads with phospholipid vesicles. C R Phys 2003;4:259–64.
[20] Le Bihan O, Bonnafous P, Marak L, Bickel T, Trepout S, Mornet S, et al. Cryo-electron tomography of nanoparticle transmigration into liposome. J Struct Biol 2009;168:419–25.
[21] Michel R, Gradzielski M. Experimental aspects of colloidal interactions in mixed systems of liposome and inorganic nanoparticle and their applications. Int J Mol Sci 2012;13:11610–42.
[22] Jaskiewicz K, Larsen A, Lieberwirth I, Koynov K, Meier W, Fytas G, et al. Probing bioinspired transport of nanoparticles into polymersomes. Angew Chem Int Ed Engl 2012;51:4613–7.
[23] Jaskiewicz K, Larsen A, Schaeffel D, Koynov K, Lieberwirth I, Fytas G, et al. Incorporation of nanoparticles into polymersomes: size and concentration effects. ACS Nano 2012;6:7254–62.
[24] Rothen-Rutishauser BM, Schuerch S, Haenni B, Kapp N, Gehr P. Interaction of fine particles and nanoparticles with red blood cells visualized with advanced microscopic techniques. Environ Sci Technol 2006;40:4353–9.
[25] Liu C, Zhen X, Wang X, Wu W, Jiang X. Cellular entry fashion of hollow milk protein spheres. Soft Matter 2011;7:11526–34.
[26] Lipowsky R, Döbereiner HG. Vesicles in contact with nanoparticles and colloids. Europhys Lett 1998;43:219–25.
[27] Deserno M, Gelbart W. Adhesion and wrapping in colloid–vesicle complexes. J Phys Chem B 2002;106:5543–52.
[28] Boulbitch A. Enforced unbinding of a bead adhering to a biomembrane by generic forces. Europhys Lett 2002;59:910–5.
[29] Deserno M, Bickel T. Wrapping of a spherical colloid by a fluid membrane. Europhys Lett 2003;62:767–73.
[30] Deserno M. Elastic deformation of a fluid membrane upon colloid binding. Phys Rev E 2004;69:031903.
[31] Fleck C, Netz R. Electrostatic colloid–membrane binding. Europhys Lett 2004;67:314–20.
[32] Gozdz WT. Deformations of lipid vesicles induced by attached spherical particles. Langmuir 2007;23:5665–9.
[33] Benoit J, Saxena A. Spherical vesicles distorted by a grafted latex bead: an exact solution. Phys Rev E 2007;76:041912.
[34] Nowak SA, Chou T. Membrane lipid segregation in endocytosis. Phys Rev E 2008;78:021908.
[35] Decuzzi P, Ferrari M. The receptor-mediated endocytosis of nonspherical particles. Biophys J 2008;94:3790–7.
[36] Chen JZY, Liu Y, Liang HJ. Structure of a tubular membrane confining spherical particles. Phys Rev Lett 2009;102:168103.
[37] Yi X, Shi X, Gao H. Cellular uptake of elastic nanoparticles. Phys Rev Lett 2011;107:098101.
[38] Cao S, Wei G, Chen JZY. Transformation of an oblate-shaped vesicle induced by an adhering spherical particle. Phys Rev E 2011;84:050901.
[39] Raatz M, Lipowsky R, Weikl TR. Cooperative wrapping of nanoparticles by membrane tubes. Soft Matter 2014. http://dx.doi.org/10.1039/c3sm52498a.
[40] Noguchi H, Takasu M. Adhesion of nanoparticles to vesicles: A Brownian dynamics simulation. Biophys J 2002;83:299–308.
[41] Smith KA, Jasnow D, Balazs AC. Designing synthetic vesicles that engulf nanoscopic particles. J Chem Phys 2007;127:084703.
[42] Fosnaric M, Iglic A, Kroll DM, May S. Monte Carlo simulations of complex formation between a mixed fluid vesicle and a charged colloid. J Chem Phys 2009;131:105103.
[43] Li Y, Gu N. Thermodynamics of charged nanoparticle adsorption on charge-neutral membranes: a simulation study. J Phys Chem B 2010;114:2749–54.
[44] Yang K, Ma Y-Q. Computer simulation of the translocation of nanoparticles with different shapes across a lipid bilayer. Nat Nanotechnol 2010;5:579–83.
[45] Vacha R, Martinez-Veracoechea FJ, Frenkel D. Receptor-mediated endocytosis of nanoparticles of various shapes. Nano Lett 2011;11:5391–5.
[46] Shi X, von dem Bussche A, Hurt RH, Kane AB, Gao H. Cell entry of one-dimensional nanomaterials occurs by tip recognition and rotation. Nat Nanotechnol 2011;6:714–9.
[47] Yue T, Zhang X. Molecular understanding of receptor-mediated membrane responses to ligand-coated nanoparticles. Soft Matter 2011;7:9104–12.
[48] Bahrami AH, Lipowsky R, Weikl TR. Tubulation and aggregation of spherical nanoparticles adsorbed on vesicles. Phys Rev Lett 2012;109:188102.
[49] Saric A, Cacciuto A. Fluid membranes can drive linear aggregation of adsorbed spherical nanoparticles. Phys Rev Lett 2012;108:118101.
[50] Saric A, Cacciuto A. Mechanism of membrane tube formation induced by adhesive nanocomponents. Phys Rev Lett 2012;109:188101.
[51] Ding H-m, Ma Y-q. Role of physicochemical properties of coating ligands in receptor-mediated endocytosis of nanoparticles. Biomaterials 2012;33(23):5798–802.
[52] Li Y, Yue T, Yang K, Zhang X. Molecular modeling of the relationship between nanoparticle shape anisotropy and endocytosis kinetics. Biomaterials 2012;33(19):4965–73.
[53] Yue T, Zhang X. Cooperative effect in receptor-mediated endocytosis of multiple nanoparticles. ACS Nano 2012;6:3196–205.
[54] Dasgupta S, Auth T, Gompper G. Wrapping of ellipsoidal nano-particles by fluid membranes. Soft Matter 2013;9:5473–82.
[55] Bahrami AH. Orientational changes and impaired internalization of ellipsoidal nanoparticles by vesicle membranes. Soft Matter 2013;9:8642–6.
[56] Dasgupta S, Auth T, Gompper G. Shape and orientation matter for the cellular uptake of nonspherical particles. Nano Lett 2014;14(2):687–93.
[57] Yue T, Wang X, Huang F, Zhang X. An unusual pathway for the membrane wrapping of rodlike nanoparticles and the orientation- and membrane wrapping-dependent nanoparticle interaction. Nanoscale 2013;5(20):9888–96.
[58] Huang C, Zhang Y, Yuan H, Gao H, Zhang S. Role of nanoparticle geometry in endocytosis: laying down to stand up. Nano Lett 2013;13(9):4546–50.
[59] Chen X, Tian F, Zhang X, Wang W. Internalization pathways of nanoparticles and their interaction with a vesicle. Soft Matter 2013;9:7592–600.
[60] Guo R, Mao J, Yan L-T. Unique dynamical approach of fully wrapping dendrimer-like soft nanoparticles by lipid bilayer membrane. ACS Nano 2013;7(12):10646–53.
[61] Yang K, Yuan B, Ma Y-q. Influence of geometric nanoparticle rotation on cellular internalization process. Nanoscale 2013;5(17):7998–8006.
[62] Yue T, Zhang X, Huang F. Membrane monolayer protrusion mediates a new nanoparticle wrapping pathway. Soft Matter 2014;10:2024–34.
[63] Champion JA, Mitragotri S. Role of target geometry in phagocytosis. Proc Natl Acad Sci U S A 2006;103(13):4930–4.
[64] Chithrani BD, Chan WCW. Elucidating the mechanism of cellular uptake and removal of protein-coated gold nanoparticles of different sizes and shapes. Nano Lett 2007;7(6):1542–50.
[65] Gratton SEA, Ropp PA, Pohlhaus PD, Luft JC, Madden VJ, Napier ME, et al. The effect of particle design on cellular internalization pathways. Proc Natl Acad Sci U S A 2008;105(33):11613–8.
[66] Jiang W, Kim BYS, Rutka JT, Chan WCW. Nanoparticle-mediated cellular response is size-dependent. Nat Nanotechnol 2008;3(3):145–50.
[67] Huang X, Teng X, Chen D, Tang F, He J. The effect of the shape of mesoporous silica nanoparticles on cellular uptake and cell function. Biomaterials 2010;31(3):438–48.
[68] Sharma G, Valenta DT, Altman Y, Harvey S, Xie H, Mitragotri S, et al. Polymer particle shape independently influences binding and internalization by macrophages. J Control Release 2010;147(3):408–12.
[69] Meng H, Yang S, Li Z, Xia T, Chen J, Ji Z, et al. Aspect ratio determines the quantity of mesoporous silica nanoparticle uptake by a small gtpase-dependent macropinocytosis mechanism. ACS Nano 2011;5(6):4434–47.
[70] Shan Y, Ma S, Nie L, Shang X, Hao X, Tang Z, et al. Size-dependent endocytosis of single gold nanoparticles. Chem Commun 2011;47(28):8091–3.
[71] Agarwal R, Singh V, Jurney P, Shi L, Sreenivasan SV, Roy K. Mammalian cells preferentially internalize hydrogel nanodiscs over nanorods and use shape-specific uptake mechanisms. Proc Natl Acad Sci U S A 2013;110(43):17247–52.
[72] Kolhar P, Anselmo AC, Gupta V, Pant K, Prabhakarpandian B, Ruoslahti E, et al. Using shape effects to target antibody-coated nanoparticles to lung and brain endothelium. Proc Natl Acad Sci U S A 2013;110(26):10753–8.
[73] Pacheco P, White D, Sulchek T. Effects of microparticle size and fc density on macrophage phagocytosis. PLoS One 2013;8(4):e60989.
[74] Yi X, Shi X, Gao H. A universal law for cell uptake of one-dimensional nanomaterials. Nano Lett 2014;14(2):1049–55.

[75] Helfrich W. Elastic properties of lipid bilayers: theory and possible experiments. Z Naturforsch C 1973;28:693–703.
[76] Seifert U, Lipowsky R. Adhesion of vesicles. Phys Rev A 1990;42:4768–71.
[77] Seifert U, Lipowsky R. Morphology of vesicles. In: Lipowsky R, Sackmann E, editors. Handbook of biological physics, vol. 1. North Holland: Elsevier; 1995.
[78] Simson R, Wallraff E, Faix J, Niewohner J, Gerisch G, Sackmann E. Membrane bending modulus and adhesion energy of wild-type and mutant cells of dictyostelium lacking talin or cortexillins. Biophys J 1998;74:514–22.
[79] Kirkpatrick S, Gelatt Jr CD, Vecchi MP. Optimization by simulated annealing. Science 1983;220:671–80.
[80] Deuling HJ, Helfrich W. The curvature elasticity of fluid membranes: a catalogue of vesicle shapes. J Phys (Paris) 1976;37:1335–45.
[81] Seifert US, Berndl K, Lipowsky R. Shape transformations of vesicles: phase diagram for spontaneous-curvature and bilayer-coupling models. Phys Rev A 1991;44(2):1182–202.
[82] R. Michel, E. Kesselmann, T. Plostica, D. Danino, M. Gradzielski, private, communication (2014).
[83] Michel R. Liposomes in contact and interacting with silica nanoparticles: from decorated vesicles to internalized particles. Göttingen: Cuvillier; 2013.
[84] Goulian M, Bruinsma R, Pincus P. Long-range forces in heterogeneous fluid membranes. Europhys Lett 1993;22:145–50.
[85] Weikl TR, Kozlov MM, Helfrich W. Interaction of conical membrane inclusions: effect of lateral tension. Phys Rev E 1998;57:6988–95.
[86] Dommersnes P, Fournier J, Galatola P. Long-range elastic forces between membrane inclusions in spherical vesicles. Europhys Lett 1998;42:233–8.
[87] Reynwar BJ, Deserno M. Membrane-mediated interactions between circular particles in the strongly curved regime. Soft Matter 2011;7:8567–75.
[88] Weikl TR. Indirect interactions of membrane-adsorbed cylinders. Eur Phys J E 2003;12:265–73.
[89] Müller MM, Deserno M, Guven J. Balancing torques in membrane-mediated interactions: exact results and numerical illustrations. Phys Rev E 2007;76:011921.
[90] Golestanian R, Goulian M, Kardar M. Fluctuation-induced interactions between rods on a membrane. Phys Rev E 1996;54:6725–34.
[91] Weikl TR. Fluctuation-induced aggregation of rigid membrane inclusions. Europhys Lett 2001;54:547–53.
[92] Lin H-K, Zandi R, Mohideen U, Pryadko LP. Fluctuation-induced forces between inclusions in a fluid membrane under tension. Phys Rev Lett 2011;107:228104.
[93] Mornet S, Lambert O, Duguet E, Brisson A. The formation of supported lipid bilayers on silica nanoparticles revealed by cryoelectron microscopy. Nano Lett 2005;5:281–5.
[94] Zhang L, Granick S. How to stabilize phospholipid liposomes (using nanoparticles). Nano Lett 2006;6(4):694–8.
[95] Yu Y, Anthony SM, Zhang L, Bae SC, Granick S. Cationic nanoparticles stabilize zwitterionic liposomes better than anionic ones. J Phys Chem C 2007;111:8233–6.
[96] Savarala S, Ahmed S, Ilies MA, Wunder SL. Stabilization of soft lipid colloids: competing effects of nanoparticle decoration and supported lipid bilayer formation. ACS Nano 2011;5(4):2619–28.
[97] Michel R, Plostica T, Abezgauz L, Danino D, Gradzielski M. Control of the stability and structure of liposomes by means of nanoparticles. Soft Matter 2013;9:4167–77.
[98] Helfrich W. Steric interaction of fluid membranes in multilayer systems. Z Naturforsch A 1978;33:305–15.
[99] Lipowsky R, Leibler S. Unbinding transitions of interacting membranes. Phys Rev Lett 1986;56:2541–4.
[100] Lynch I, Dawson KA. Protein–nanoparticle interactions. Nano Today 2008;3:40–7.
[101] Monopoli MP, Walczyk D, Campbell A, Elia G, Lynch I, Bombelli FB, et al. Physical–chemical aspects of protein corona: relevance to in vitro and in vivo biological impacts of nanoparticles. J Am Chem Soc 2011;133(8):2525–34.
[102] Weikl TR, Asfaw M, Krobath H, Różycki B, Lipowsky R. Adhesion of membranes via receptor–ligand complexes: domain formation, binding cooperativity, and active processes. Soft Matter 2009;5:3213–24.
[103] Hu J, Lipowsky R, Weikl TR. Binding constants of membrane-anchored receptors and ligands depend strongly on the nanoscale roughness of membranes. Proc Natl Acad Sci U S A 2013;110(38):15283–8.
[104] Li Y, Chen X, Gu N. Computational investigation of interaction between nanoparticles and membranes: hydrophobic/hydrophilic effect. J Phys Chem B 2008;112(51):16647–53.
[105] Curtis EM. A novel, systematic multiscale modeling method to calculate coarse-grained parameters for the simulation of biomolecules. (Doctoral dissertation) Raleigh, North Carolina: North Carolina State University; 2013.
[106] Curtis EM, Hall CK. Molecular dynamics simulations of DPPC bilayers using “LIME”, a new coarse-grained model. J Phys Chem B 2013;117(17):5019–30.